10. HUMAN CONTRIBUTION TO THE RECORD SUNSHINE OF WINTER 2014/15 IN THE UNITED KINGDOM

Nikolaos Christidis, Mark McCarthy, Andrew Ciavarella, and Peter A. Stott

Extreme winter sunshine in the United Kingdom, as observed in the record high 2014/15 season, has become more than 1.5 times more likely to occur under the influence of anthropogenic forcings.

Observational data of sunshine duration since 1930 from the Met Office National Climate Information Centre (NCIC; Perry and Hollis 2005) reveal that winter 2014/15 was the sunniest in the United Kingdom (Fig. 10.1a). The common perception of drab British winters is seemingly challenged by the increasing trend of 2.4 ± 0.7 sunshine hrs decade^{-1} (mean ± standard deviation) during 1930–2015 (Fig. 10.1a). With winters in the region projected to become warmer and wetter in a changing climate (van Oldenborgh et al. 2013), increasing sunshine would suggest longer sunny spells between heavier rainfall events. Brighter winters may also enhance solar energy production. Annual sunshine over western Europe was found to follow periods of dimming in the 1960–80s and brightening thereafter, while large positive seasonal trends are particularly evident in winter (Sanchez-Lorenzo et al. 2008). Contrary to the changes in Europe, a sunshine decline in recent decades has been observed in parts of the world where aerosol concentrations have been increasing, such as China and the Indian subcontinent (Wang et al. 2012; Liao et al. 2015; Niroula et al. 2015).

We attempt to formally establish the role of the overall anthropogenic forcing on the climate based on ensembles of simulations with and without anthropogenic effects produced with an atmospheric model. This well-established methodology (Pall et al. 2011; Christidis et al. 2013) provides distributions of climatic variables in the actual (ALL forcings) and natural (NAT) climate, constructed with the two ensembles. Probabilities P_1 and P_0 of a threshold exceedance computed with the ALL and NAT simulations help assess the anthropogenic effect in terms of the fraction of attributable risk (FAR; Allen 2003), defined as $1 - (P_0 / P_1)$. FAR values close to unity indicate prominent human influence on the event. Changes in the return time of extreme events (estimated from inverse probabilities) can also be examined.

AFFILIATIONS: Christidis, McCarthy, Ciavarella, and Stott—Met Office Hadley Centre, Exeter, United Kingdom

DOI:10.1175/BAMS-D-16-0143.1

A supplement to this article is available online (10.1175/BAMS-D-16-0143.2)

As models do not provide a sunshine duration diagnostic, we employ the downward solar (SW) flux at the surface as a proxy (Fig. 10.1a). Observed winter sunshine hours and solar radiation averaged over the United Kingdom have a correlation of 0.9 over the common observational period, though individual years may differ in sign of anomaly (e.g., 2010). Cloud cover (correlation coefficient 0.3 for inverse variable estimated from observations) would be less suitable in our analysis, as it also incorporates a nighttime component. SW winter flux in 2014/15 is a joint record together with 2007/08, though flux observations cover a considerably shorter period than sunshine.

We employed the Hadley Centre event attribution system (Christidis et al. 2013), built on the HadGEM3–A model, to generate the ALL and NAT simulations. A major upgrade of the model was recently undertaken within the EUCLEIA project (http://eucleia.eu/). As a result, our system now features the highest resolution model used in attribution studies, with 85 vertical levels and about 60-km horizontal resolution. Ensembles of 15 simulations were produced for both the ALL and NAT experiments, which cover the period 1960–2013. Observed sea surface temperatures (SSTs) and sea ice data (Rayner et al. 2003) were used as boundary conditions in the ALL simulations. An estimate of the anthropogenic warming in the SSTs obtained from atmosphere–ocean coupled models (Stone 2013) was subtracted from the SST observations in the NAT simulations and the sea ice was adjusted accordingly (Christidis et al. 2013). Figure 10.1b depicts the modeled time series of the SW winter flux anomaly relative to 1961–90 corresponding to the ensemble

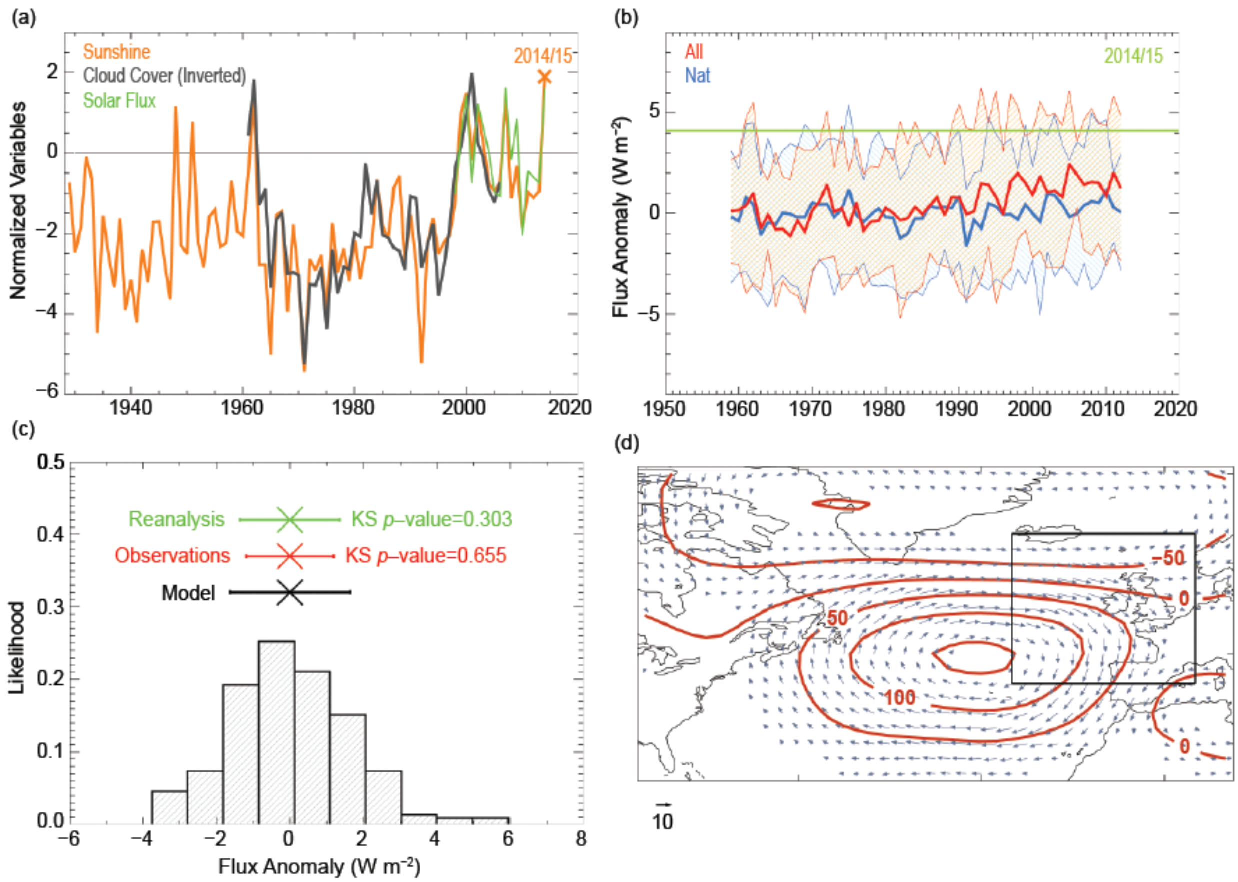

Fig. 10.1. (a) U.K. winter sunshine (orange), inverted cloud cover (gray), and solar flux (green) time series constructed with NCIC observations and normalized relative to the common observational period. (b) Time series of winter flux anomalies relative to 1961–90 from the ALL (red) and NAT (blue) experiments. The thick lines correspond to the ensemble mean, and the thin lines mark the ± 2 standard deviation range. The 2014/15 anomaly estimate is shown in green. (c) Modeled flux anomalies in recent winters (histogram) and the ± 1 standard deviation range from different datasets (whiskers). KS tests examine whether the modeled data are significantly different from the other datasets. (d) Winter mean geopotential height (red) and wind (blue arrows) anomalies relative to 1961–90 at 500 hPa constructed with reanalysis data.

mean of the two experiments, together with their ± 2 standard deviation (SD) range. An increase relative to the natural world becomes evident after the 1990s. The 2014/15 flux was 1.55 times above the mean during the observational period (1998–2012), which corresponds to an anomaly estimate of 4.1 W m^{-2} (green line in Fig. 10.1b). This estimate is subsequently used as a threshold to calculate the probabilities of extreme events P_1 and P_0.

Modeled fluxes for the actual climate are evaluated against NCIC observations and data from the NCEP–NCAR reanalysis (Kalnay et al. 1996). We select the common winters in the three datasets and using anomalies relative to the common period mean, we conduct two-sided Kolmogorov–Smirnov (KS) tests that show no significant difference between the simulated fluxes and the reanalysis or observational data (P values greater than 0.1; Fig. 10.1c). The good agreement remains when the model is evaluated over a longer period against the reanalysis (which includes more years than the observations).

Apart from the role of anthropogenic climate change, the possible contribution from the atmospheric flow in winter 2014/15 to the extreme sunshine will also be considered in our study (Fig. 10.1d). Synoptic conditions are often crucial to the occurrence of extremes (Wallace et al. 2015; Deser et al. 2012). For example, a persistent southwesterly flow over the United Kingdom was a key factor to the extreme rainfall in the winter before the one examined in this study (Christidis and Stott 2015). Figure 10.1d illustrates a predominantly zonal westerly flow in winter 2014/15 (also seen in the surface pressure pattern and consistent with the observed positive phase of the North Atlantic Oscillation), which transports moist air over the United Kingdom and would not generally be expected to provide favorable conditions for sunshine. The warming ocean seen in SST observations would also not favor extreme sunshine, as it increases the amount of water vapor in the atmosphere. The observed 2014/15 winter mean SST over the wider U.K. region is close to its mean value after 1980 when the sunshine increases and is therefore unlikely to have influenced the event.

Results. We first estimate the return time corresponding to the 2014/15 solar flux anomaly and investigate how it has changed in the present climate relative to the natural world, irrespective of the atmospheric circulation (i.e., under any synoptic conditions). We use the winters of the most recent simulated decade (2004–13) as a proxy of the present climate (i.e., 150 seasons for each experiment) and construct distributions of the solar flux anomaly with and without human influence. Estimates of P_1 and P_0 are then obtained from the two distributions using the generalized Pareto distribution, while uncertainties are derived with a Monte Carlo bootstrap procedure (Christidis et al. 2013). In that way, we construct the return time (inverse probability) distributions shown in Fig. 10.2a. The results indicate that anthropogenic forcings lead to a marked decrease in the return time from 48 to 14 years (best estimates, defined as the 50th percentile of the distributions). The distribution of the FAR is shown in Fig 10.2b. The best estimate of the FAR is 0.72, suggesting that human influence increases the chances of extreme events by a factor of 3.6 (5%–95% uncertainty range: 1.6–17.2). We also examine how the chances have changed in consecutive decades since the 1960s (Fig. 10.2c). The return time decreases from over a century in the mid-1960s to about 15 years after the mid-1990s and remains well below the NAT estimates in the last 20 years.

To assess the effect of the atmospheric circulation, we adopt the approach of Christidis and Stott (2015), whereby we partition the simulated winters between those that resemble the reference flow pattern (Fig. 10.1d) and those that do not. The grouping is based on the correlation coefficient over the wider U.K. region marked by the box in Fig. 10.1d. To separate the circulation effect from that of anthropogenic forcings, we only use the NAT simulations, which yield a total of 810 winters, 197 of which belong to the high-correlation group with correlation coefficients above 0.6. The mean flow of the highly correlated seasons resembles the reanalysis pattern, whereas the mean of winters with low correlations displays a weak easterly flow (see online supplemental material).

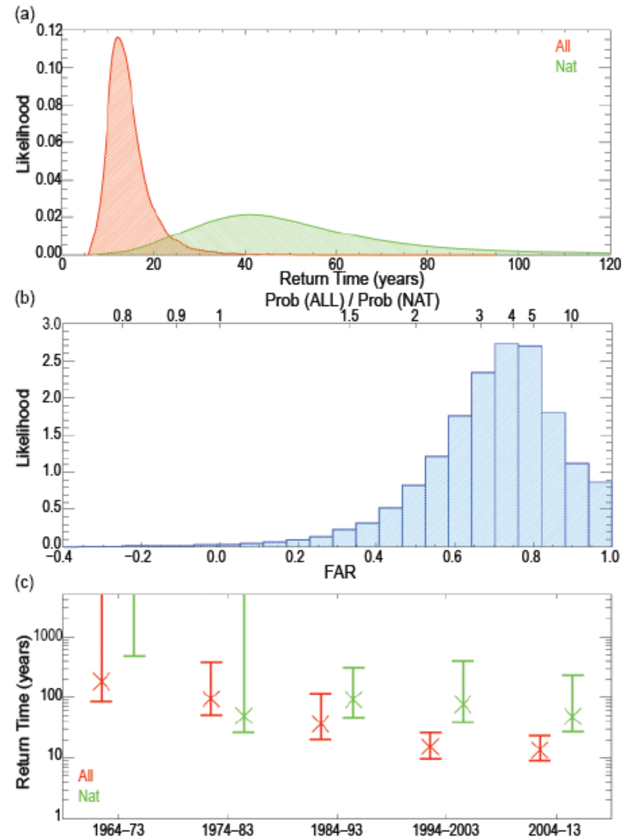

Fig. 10.2. (a) Normalized distributions of the return time of an extreme winter sunshine event in the United Kingdom, defined as an exceedance of the 2014/15 solar flux anomaly. The distributions were constructed with (red) and without (green) anthropogenic climate change. (b) Normalized FAR distribution measuring how much human influence changes the likelihood of an extreme winter sunshine event. The change in probability is shown on the top x axis. (c) Change in the return time of extreme events with (red) and without (green) anthropogenic climate change in consecutive decades. The best estimate (50th percentile) is represented by the cross, and the 5%–95% uncertainty range is marked by the whiskers.

The latter is associated with colder and drier continental air over the United Kingdom, which is more conducive to sunny conditions. Indeed, we find that winters with low-pattern correlations are about 14 times more likely to break the 2014/15 flux record (5%–95% uncertainty range: 3.7 to >10^3). Our findings are not too sensitive to the choice of the correlation coefficient used to discriminate between seasons (see online supplemental material).

Conclusions. Evidence of human influence on winter sunshine extremes in the United Kingdom is shown here, consistent with an observed increasing trend in sunshine hours in recent decades. This trend together with internal variability appear to have been key drivers of the 2014/15 record, which occurred within a meteorological context not typical of sunny conditions. Changes in aerosol emissions constitute the component of the anthropogenic forcing most likely to affect sunshine (Sanchez-Romero et al. 2014). Unlike winter, NCIC observations do not show a notable trend in summer sunshine, when one might expect the direct effect from reduced aerosol concentrations to be larger due to the decreased cloud amount. The discrepancy might be a result of the indirect effect linked to changes in cloud properties that could be stronger in winter, though this needs to be further investigated in future work.

ACKNOWLEDGEMENTS. This work was supported by the Joint BEIS/Defra Met Office Hadley Centre Climate Programme (GA01101) and the EUCLEIA project funded by the European Union's Seventh Framework Programme [FP7/2007-2013] under Grant Agreement No. 607085.

REFERENCES

Allen, M. R., 2003: Liability for climate change. *Nature*, **421**, 892.

Christidis, N., and P. A. Stott, 2015: Extreme rainfall in the United Kingdom during winter 2013/2014: The role of atmospheric circulation and climate change [in "Explaining Extremes of 2014 from a Climate Perspective"]. *Bull. Amer. Meteor. Soc.*, **96 (12)**, S46–S50, doi:10.1175/BAMS-D-15-00094.1.

——, ——, A. Scaife, A. Arribas, G. S. Jones, D. Copsey, J. R. Knight, and W. J. Tennant, 2013: A new HadGEM3-A based system for attribution of weather and climate-related extreme events. *J. Climate*, **26**, 2756–2783, doi:10.1175/JCLI-D-12-00169.1.

Deser, C., R. Knutti, S. Solomon, and A. S. Phillips, 2012: Communication of the role of natural variability in future North American Climate. *Nat. Climate Change*, **2**, 775–779, doi:10.1038/nclimate1562.

Kalnay, E., and Coauthors, 1996: The NCEP/NCAR 40-year reanalysis project. *Bull. Amer. Meteor. Soc.*, **77**, 437–470.

Liao, W., X. Wang, Q. Fan, S. Zhou, M. Chang, Z. Wang, Y. Wang, and Q. Tu, 2015: Long-term atmospheric visibility, sunshine duration and precipitation trends in South China. *Atmos. Environ.*, **107**, 204–2016, doi:10.1016/j.atmosenv.2015.02.015.

Niroula, N., K. Kobayashi, and J. Xu, 2015: Sunshine duration is declining in Nepal across the period from 1987 to 2010. *J. Agric. Meteor.*, **71**, 15–23, doi:10.2480/agrmet.D-14-00025.

Pall, P., T. Aina, D. A. Stone, P. A. Stott, T. Nozawa, A. G. J. Hilberts, D. Lohmann, and M. R. Allen, 2011: Anthropogenic greenhouse gas contribution to flood risk in England and Wales in autumn 2000. *Nature*, **470**, 382–385, doi:10.1038/nature09762.

Perry, M., and D. Hollis, 2005: The generation of monthly gridded datasets for a range of climatic variables over the UK. *Int. J. Climatol.*, **25**, 1041–1054, doi:10.1002/joc.1161.

Rayner, N. A., D. E. Parker, E. B. Horton, C. K. Folland, L. V. Alexander, D. P. Rowell, E. C. Kent, and A. Kaplan, 2003: Global analyses of sea surface temperature, sea ice, and night marine air temperature since the late nineteenth century. *J. Geophys. Res.*, **108**, 4407, doi:10.1029/2002JD002670.

Sanchez-Lorenzo, A., J. Calbó, and J. Martin-Vide, 2008: Spatial and temporal trends in sunshine duration over western Europe (1938–2004). *J. Climate*, **21**, 6089–6098, doi:10.1175/2008JCLI2442.1.

Sanchez-Romero, A., A. Sanchez-Lorenzo, J. Calbó, J. A. González, and C. Azorin-Molina, 2014: The signal of aerosol-induced changes in sunshine duration records: A review of the evidence. *J. Geophys. Res. Atmos.*, **119**, 4657–4673,doi:10.1002/2013JD021393.

Stone, D., 2013: Boundary conditions for the C20C Detection and Attribution Project: The All-Hist/est1 and Nat-Hist/CMIP5-est1 scenarios. Lawrence Berkeley National Laboratory, 18 pp. [Available online at http://portal.nersc.gov/c20c/input_data/C20C-DandA_dSSTs_All-Hist-est1_Nat-Hist-CMIP5-est1.pdf.]

Van Oldenborgh, G. J., M. Collins, J. Arblaster, J. H. Christensen, J. Marotzke, S. B. Power, M. Rummukainen, and T. Zhou, 2103: Annex I: Atlas of global and regional climate projections. *Climate Change 2013: The Physical Basis,* T. F. Stocker et al., Eds., Cambridge University Press, 1311–1393.

Wallace, J. M., C. Deser, B. V. Smoliak, and A. S. Philips, 2015: Attribution of climate change in the presence of internal variability. *Climate Change: Multidecadal and Beyond*, C.-P. Chang et al., Eds., World Scientific, 1–29.

Wang, Y., Y. Yang, N. Zhao, C. Liu, and Q. Wang, 2012: The magnitude of the effect of air pollution on sunshine hours in China. *J. Geophys. Res.*, **117**, D00V14, doi:10.1029/2011JD016753.